

A robust method, based on a novel source, for performance and diagnostic capabilities assessment of the positron emission tomography system

Alexandros P. Samartzis¹ MSc,
George P. Fountos² PhD,
Ioannis S. Kandarakis² PhD,
Evangelia P. Kounadi³ PhD,
Emmanuel N. Zoros¹ MSc,
Evangelia Skoura¹ MD, PhD,
Ioannis E. Datseris¹ MD, PhD,
George H. Nikiforides⁴ PhD.

1. Nuclear Medicine Department, "Evangelismos" General Hospital, Ypsilantou 45-47, 10676, Athens, Greece.

2. Technological Educational Institute (T.E.I.) of Athens/ Department of Medical Instruments Technology, Ag. Spyridonos, 12210, Athens, Greece.

3. Department of Medical Physics, "Alexandra" General Hospital, Vasilisis Sofias 80, 11528, Athens, Greece.

4. Department of Medical Physics, Faculty of Medicine, University of Patras, 265 00 Patras, Greece.

Keywords: Positron emission tomography
 - Spatial resolution
 - Modulation transfer function
 - Line spread function - Point spread function
 - Plane source

Correspondence address:

Assoc. Prof. Dr. G. Fountos
 Department of Medical Instruments Technology,
 Technological Educational Institute of Athens,
 Ag. Spyridonos Street, Egaleo, 12210, Athens, Greece.
 Tel: (+30210) 5385-375 (work)
 E-mail: gfoun@teiath.gr

Received:

1 June 2014

Accepted revised:

14 July 2014

Abstract

The aim of our work was to provide a robust method for evaluating imaging performance of positron emission tomography (PET) systems and particularly to estimate the modulation transfer function (MTF) using the line spread function (LSF) method. A novel plane source was prepared using thin layer chromatography (TLC) of a fluorine-18-fluorodeoxyglucose (¹⁸F-FDG) solution. The source was placed within a phantom, and imaged using the whole body (WB) two dimensional (2D) and three dimensional (3D) standard imaging protocols in a GE Discovery ST hybrid PET/CT scanner. Modulation transfer function was evaluated by determining the LSF, for various reconstruction methods and filters. The proposed MTF measurement method was validated against the conventional method, based on point spread function (PSF). Higher MTF values were obtained with 3D scanning protocol and 3D iterative reconstruction algorithm. All MTF obtained using 3D reconstruction algorithms showed better preservation of higher frequencies than the 2D algorithms. They also exhibited better contrast and resolution. MTF derived from LSF were more precise compared with those obtained from PSF since their reproducibility was better in all cases, providing a mean standard deviation of 0.0043, in contrary to the PSF method which gave 0.0405. *In conclusion*, the proposed method is novel and easy to implement for characterization of the signal transfer properties and image quality of PET/computed tomography (CT) systems. It provides an easy way to evaluate the frequency response of each kernel available. The proposed method requires cheap and easily accessible materials, available to the medical physicist in the nuclear medicine department. Furthermore, it is robust to aliasing and since this method is based on the LSF, is more resilient to noise due to greater data averaging than conventional PSF-integration techniques.

Hell J Nucl Med 2014; 17(2): 97-105

Published online: 7 August 2014

Introduction

Positron emission tomography (PET) is a powerful molecular imaging modality enabling measurements of radiotracers distributions in vivo. Spatial resolution is the ability of the system to image an object without blurring and so, it is a measure of how close two adjacent objects can be distinguished. The spatial resolution is usually characterized by the modulation transfer function (MTF), which reports the amount of sinusoidal signals transferred by the imaging system [1]. Positron emission tomography imaging is affected by a number of resolution degrading factors that include random positron range, photon pair noncollinearity attenuation, intercrystal penetration, intercrystal scatter, detector inefficiencies, and electronics mispositioning. In total, a PET system has a spatially variant resolution loss [2]. Evaluation of imaging system performance has a long history and many attempts have been made to characterize tomographic imaging systems by combining factors that describe each component into one figure of merit. The signal spread of an imaging system can be described by the point spread function (PSF) or the line spread function (LSF). The full width at half maximum (FWHM) of these functions is the most used measure for assessing the resolution of a system. However, FWHM lacks the possibility to completely characterize these systems since different LSF or PSF shapes may show equal FWHM values [3, 4]. An alternative is to use the MTF in order to describe the ability of a system to maintain the amplitudes of spatial frequencies passing through it [5-9]. Precise and accurate determinations of MTF are important for comparing the effects of different scan and reconstruction parameters, for comparison between different PET scanners and specifically for evaluating the accuracy of size and density measurements of fine details in medical images [10-14].

The objective of this work was to provide a measurement method for evaluating resolution performance of PET systems and particularly to estimate the MTF using the LSF method. MTF determination by use of LSF has been previously presented in the literature [15-17]. The key to our approach was the preparation of a novel and highly homogeneous-

plane source, based on fluorine-18-fluorodeoxyglucose (^{18}F -FDG) as the positrons emitting radiopharmaceutical and subsequently its two gamma 511 keV photons. The advantage of this test-object (the thin plane source) is that it can be prepared by using materials easily accessible in a hospital environment. The above introduces a low cost method that could be used for evaluating task-based resolution metrics for system optimization and comparison across standard and iterative reconstruction algorithms, as well as for comparison of different PET systems and routine quality control. Clinical scanning protocols could also be evaluated. In conclusion, the use of MTF provides a common language between physicians and physicists, as a mean to quantify image quality.

Materials and methods

The method for estimation of MTF in PET systems, presented in this study, is based on the determination of LSF from cross sectional images of a thin plane source. An integrated PET/CT system (GE, Discovery ST PET/CT, Milwaukee, WI) was used to demonstrate the proposed method. The plane source was prepared in our laboratory by thin layer chromatography of a radiopharmaceutical solution. A custom software, that incorporates the functionality of estimating the MTF from both LSF and PSF, was also developed.

Preparation of the MTF test object

Preparation of a film-based plane source for the LSF measurement
It has been demonstrated in the literature that several ways can be used to create phantoms in nuclear medicine [18]. The use of chromatography paper to produce a radioactive thin plane source has not been implemented previously. For this study, a novel plane source was prepared by immersing Al substrate chromatography paper (Al foils 5×10cm coated with silica gel, Fluka), in a radioactive solution. The radioactive solution was prepared by adding ~120MBq of the radiopharmaceutical ^{18}F -FDG into 50mL of $\text{CH}_3\text{CN}/\text{NaCl}$ (95:5). The $\text{CH}_3\text{CN}/\text{NaCl}$ is the solvent of the process. For the incubation of the chromatography plate with the radiopharmaceutical solution, a 250mL glass beaker has been used. The chromatography plate was placed vertically, with less than 1cm immersed, in the solution for 10 to 15min. At the end of incubation, the chromatography paper was examined optically for the optimum adsorption-binding of the solution onto the substrate and left to dry for 15min. Stripes of 1cm from the bottom and the upper part of the chromatography paper were cut off, to avoid any inconsistency in the radioactivity distribution. The plane source resulted exhibits an activity of 2.85MBq, as measured with an Atomlab 300 (Biodex Medical Systems) dose calibrator.

The source was sandwiched in the center of eight, 1cm thick, 10×12.5cm poly(methyl-methacrylate) (PMMA) slabs and imaged in a General Electric Discovery ST, PET/CT scanner, as shown in Figure 1. The coronal image of the source (matrix: 256×256) was carefully reviewed for in-homogeneities in the radioactivity distribution for the MTF evaluation of PET images. The uniformity was also evaluated by obtaining regions of interest (ROI) on the coronal slice of the source while placed horizontally on the scanner bed. The

source exhibits a maximum non-uniformity deviation of 4.3%. The reconstructed PET images, with the phantom placed in the horizontal and vertical direction, are shown in Figure 2.

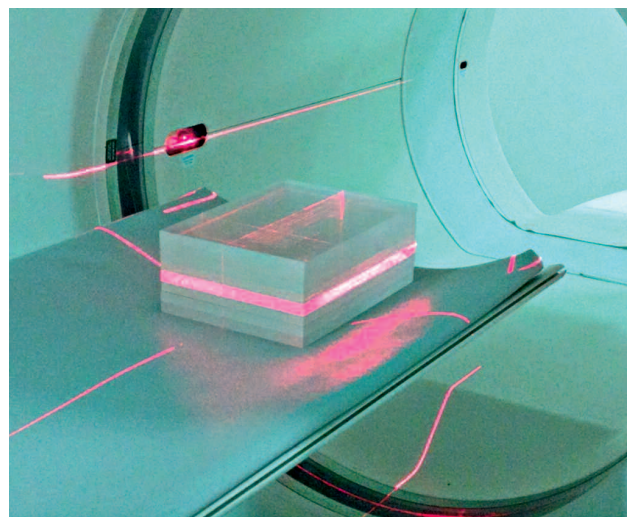


Figure 1. The PMMA blocks with the plane source inside placed on the bed of the GE Discovery ST PET/CT.

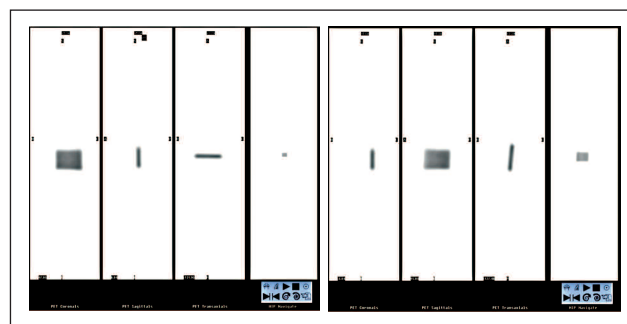


Figure 2. Left: Coronal, sagittal and transverse slices of the phantom, when the plane source is placed in parallel to coronal direction (i.e. horizontally). Right: Coronal, sagittal and transverse slices of the phantom, when the plane source is placed in parallel to sagittal direction (i.e. vertically).

Preparation of the point source for the PSF measurement

In order to prepare a point source, the following procedure was followed: A micro pipette was used to place a sample of ^{18}F -FDG with >200MBq/cc (5mCi/cc) activity concentration on a slide. The end of a hematocrit capillary tube (1mm internal diameter capillary glass tube), was placed onto the drop. The capillary action draws the drop into the tube. Care was taken for the prepared source to be less than 1mm in axial length. If the source is longer than 1mm, the measured axial resolution will increase. Both ends of the tube were sealed with sodium bentonite clay, with the end of the tube with activity sealed first [4].

The capillary tube was fitted to the center of the field of view (FOV) of the scanner as shown in Figure 3 and imaged with a 20cm diameter FOV, matrix 256×256. A transverse slice image of the point source is also shown in Figure 3.

MTF

The MTF was obtained by using both the LSF and PSF methods, for the 2D and 3D PET/CT imaging protocols, after appli-

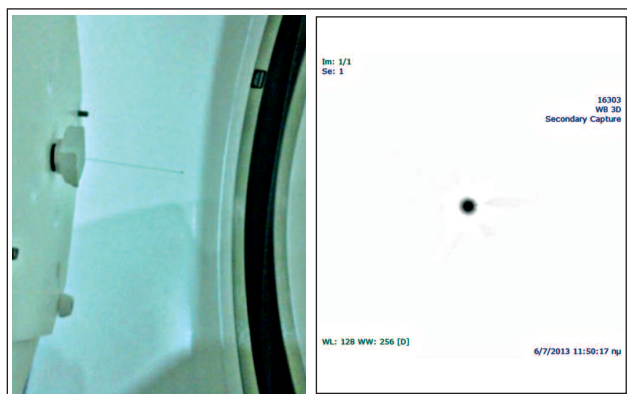


Figure 3. Left: The point source placed in the center of the FOV of the scanner. Right: Transverse slice image of the point source.

cation of various reconstruction and filtering algorithms on the thin plane (LSF) and point source (PSF) images, for comparison purposes. The reconstruction algorithms used, were the ones installed in the dimension console of the Discovery ST, PET/CT system (Milwaukee, WI).

The smallest displayed FOV, appropriate to the phantom dimensions, was used as otherwise the postsampling pixel pitch (of the image display matrix) may limit the resolution and affect the MTF computation [8]. Because a small display FOV is desired, the dimensions of the phantom should also be relatively small. The 8cm thick by 12.5cm long phantom used in this study was well suited to a FOV with 20cm diameter [6].

LSF

In the LSF method, the phantom with the thin plane source was placed in the center of the field of view with slight horizontal angulation. In this study, the angle of the line relative to the horizontal was measured as 1.6°. However, as with the Fujita technique, angles spanning from approximately 1° to 8° are generally useful. For angles >8°, the dimensions of the vertical LSF differ from those of the true LSF by more than 1%, and geometrical corrections should be considered. The final LSF was obtained by averaging all line LSF profiles after angle correction. The angle correction was performed following the procedure described in Fountos et al [12]. The line LSF profile can be written as $LSF(\xi) = G(x_i, y_i)$, where $G(x_i, y_i)$ represents the slit ROI image pixel values, x_i, y_i are the pixel coordinates in the horizontal and vertical axes respectively, ranging as follows $x_1 \leq x_i \leq x_2, y_1 \leq y_i \leq y_2$. x_1, x_2 define the range, where each line LSF was calculated and y_1, y_2 are the corresponding lengths. The average LSF profile was calculated as [19]:

$$LSF(\xi) = \frac{\sum_{x_i=x_1}^{x_2} \sum_{y_i=y_1}^{y_2} y_i G(x_i, y_i)}{\sum_{x_i=x_1}^{x_2} \sum_{y_i=y_1}^{y_2} y_i l} \quad (1)$$

where $\xi = \tan(\theta)$, x_i, y_i , and θ is the angle between the line image and the horizontal or vertical axis.

Since the plane source could have been positioned, either clockwise or counter clockwise, in a slight angle ranging from -80 to -10 and 10 to 80, a custom made software devel-

oped in Matlab (MathWorks, Natick, MA) was used for angle correction [12]. The software is testing negative and positive angles and for each angle it calculates the corrected averaged LSF and standard deviation (sd) for all data points. The angle showing the minimum average sd is adopted as the optimum angle and it was then used for correction. The average LSF was fitted using four different functions: i) a Gaussian function, ii) a sum of two Gaussian functions, iii) a Lorentzian function and iv) a hybrid (sum of a Gaussian and a Lorentzian) function, in order to reduce noise in the LSF, which could result in MTF overestimation [19-22]. The fitting function providing the optimum correlation coefficient (R^2) was selected. Fourier transformation and subsequent normalization were then applied on the final LSF to compute the MTF [7, 8, 12].

PSF

MTF was also obtained through the PSF method similar to the one described in Fountos et al [12]. The center of the point image was determined (x_0, y_0 coordinates) and line profiles passing from this point were obtained covering various angles ranging from 00 to 1800 with a 20 angle step.

The PSF profile can be written as $PSF(\xi) = G(x_i, y_i)$ where $G(x_i, y_i)$ are the image pixel values [15]. x_i, y_i are the pixel coordinates in the horizontal and vertical axes respectively, fulfilling the line equation criteria for the following equation:

$$y = \frac{y_2 - y_1}{x_2 - x_1} (x - x_1) + y_1$$

Where: $x_1 = x_0 + r \cdot \sin \theta, x_2 = x_0 - r \cdot \sin \theta, y_1 = y_0 - r \cdot \cos \theta, y_2 = y_0 + r \cdot \cos \theta$ with $0^\circ \leq \theta \leq 180^\circ$ and r is the half length of the line profile.

Almost all applications of the PSF, as a generalized descriptor of tomographic systems performance, follow the assumption of rotational symmetry [12, 23-29], therefore the PSF profiles in the radial directions can be averaged to produce a one dimensional (1D) PSF profile, which was calculated as [30]:

$$PSF(\xi) = \frac{\sum_{x_i=x_1}^{x_2} \sum_{y_i=y_1}^{y_2} G(x_i, y_i)}{\sum_{x_i=x_1}^{x_2} \sum_{y_i=y_1}^{y_2} l} \quad (3)$$

Where ξ is the pixel position in horizontal axis. The MTF was then calculated as described in the LSF method (see section B.1).

Goodness of fit

To evaluate the goodness of fit, in the LSF and PSF fitting approaches, the correlation coefficient (R^2) and the root mean square error (RMSE) were calculated.

The RMSE was used as a measure of goodness of fit between the fitted and the measured values [31]. The differences between measured and fitted values are also called residuals, and the RMSE serves to aggregate them into a single measure of predictive power. The RMSE of the fitted values with respect to the measured ones is defined as the square root of the mean squared error, according to the following equation (4):

$$RMSE = \sqrt{\frac{\sum_{i=1}^n (x_{m,i} - x_{f,i})^2}{n(n-1)}} \quad (4)$$

Where $x_{m,i}$ is the measured values and $x_{f,i}$ is the fitted values at i .

MTF reproducibility, for both LSF and PSF methods, was determined by repeating MTFs calculation ten times, yielding the mean sd .

Results

Figures 4 and 5, show line spread functions (LSF) obtained by the LSF and by the PSF methods respectively, fitted with the Gaussian, the summation of two Gaussians, the Lorentzian and the hybrid Gaussian & Lorentzian functions. The LSFs were obtained with the standard WB PET 3D protocol with 3D reconstruction method: iterative, 21 subsets, 2 iterations. The PSF were obtained in 3D mode with 3D reconstruction method: FORE FBP and transaxial filter Ramp with minimum cut-off 6.4mm.

The values of R^2 and RMSE for the different fitting functions are shown in Table 1, for both LSF and PSF methods. These values were used as a criterion for the selection of the optimum fitting function used in the subsequent MTF calculation.

For the 3D scanning mode (i.e. without septa), Figure 6 plots the MTF of different reconstruction algorithms. The algorithms were: 1) iterative, 2) FORE iterative, 3) FORE filtered back projection and 4) Reprojection. The advance of the fully 3D iterative reconstruction algorithm is clearly shown by its MTF. Compared with the two Fourier rebinding (FORE iterative and FORE filtered back projection) as well as the reprojection algorithms, iterative reconstruction exhibits increased contrast. That is so the case because high MTF values in the low frequency range are needed to outline the coarse details of the image and is important for presentation and detection of relatively large but low contrast lesions. Consequently increased MTF values in the high frequency range are necessary to portray fine details and sharp edges. This is of obvious importance for small objects and also sometimes for larger objects because of the importance of edges and sharp bor-

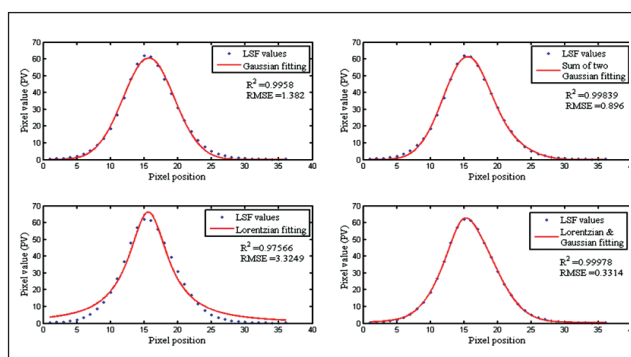


Figure 4. Representation of the four fitting methods to the averaged line spread function (LSF) values for the PET image obtained with the PETWB 3D imaging protocol and 3D Reconstruction method: Iterative with 21 subsets and 5 iterations. Top left: Gaussian. Top right: Sum of two Gaussians. Bottom left: Lorentzian. Bottom right: Hybrid Gaussian & Lorentzian (LSF/MTF method).

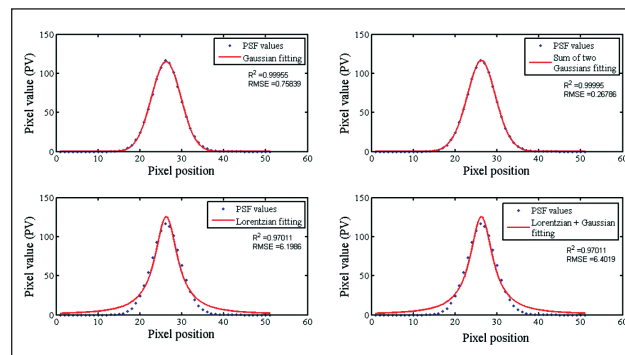


Figure 5. Representation of the four fitting methods to the averaged point spread function (PSF) values for the PET image obtained with the PET WB 3D imaging protocol and 3D Reconstruction method: FORE FBP and transaxial filter ramp with minimum cut-off 6.4mm. Top right: Sum of two Gaussians. Bottom left: Lorentzian. Bottom right: Hybrid Gaussian & Lorentzian (PSF/MTF method).

Table 1. Goodness of fit for the LSF and PSF methods shown in Figures 4 and 5

Fitting results for the LSF & PSF methods		Goodness of fit parameters		Fitting
PET Protocol	Reconstruction method	RMSE	(R^2)	
LSF (3D)	Iterative	1.382	0.9958	Gaussian
	(21 subsets, 2 iterations)	0.896	0.9984	Sum of two Gaussians
		3.324	0.9757	Lorentzian
		0.331	0.9998	Hybrid Gaussian & Lorentzian
PSF (3D)	FORE FBP	2.1583	0.9897	Gaussian
	Transaxial filter:	0.3375	0.9998	Sum of two Gaussians
	Ramp cut-off =6.4mm	2.6422	0.9846	Lorentzian
		0.6287	0.9993	Hybrid Gaussian & Lorentzian

ders for the detection of low contrast objects and for accurate assessment of their size and shape.

For the 3D scanning mode, Figures 7 and 8 demonstrate the effect into the MTF from different iterations and different subsets, respectively. In Figure 7, the reconstruction algorithm used was iterative with 21 subsets and the iterations were 2, 4, and 6. In Figure 8, the reconstruction algorithm was iterative with 2 iterations, while subsets ranged from 10 to 35.

For the 2D scanning mode (i.e. with septa), Figure 9 demonstrates the effect of different filters to the MTF. The 2D reconstruction method was back projection and the filters chosen were: Hanning, Ramp, Shepp Logan, Butterworth 2 and Enhanced Hanning.

Figures 10 and 11 plot MTF obtained with 2D OS EM reconstruction and show the effect of different iterations and subsets. For Figure 10, the reconstruction algorithm used was OS EM with 21 subsets and the iterations were 2, 4, and

Original Article

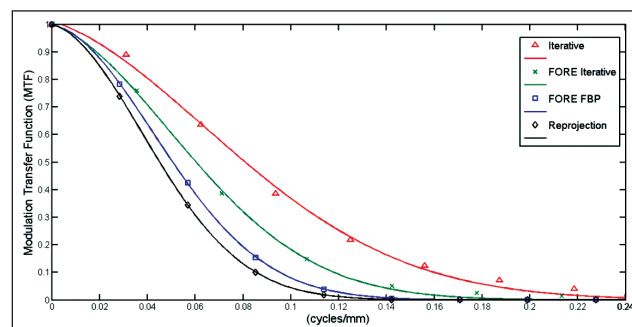


Figure 6. Modulation transfer function, obtained with the LSF method from PET images using the plane source method and 3D scanning with different reconstruction algorithms. The algorithms are: 1) iterative, 2) FORE iterative, 3) FORE filtered back projection and 4) Reprojection.

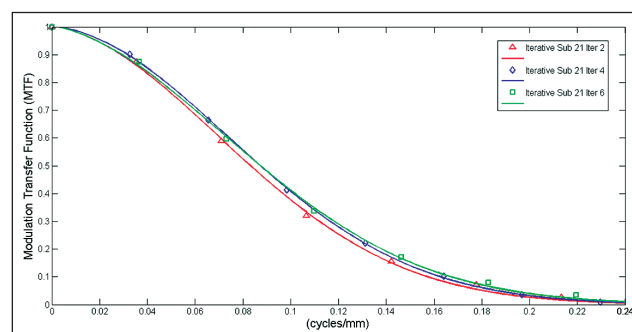


Figure 7. 3D scanning and the effect of different iterations into the MTF. MTF obtained with the LSF method from PET images using the plane source method, 3D scanning and iterative reconstruction algorithm with 21 subsets.

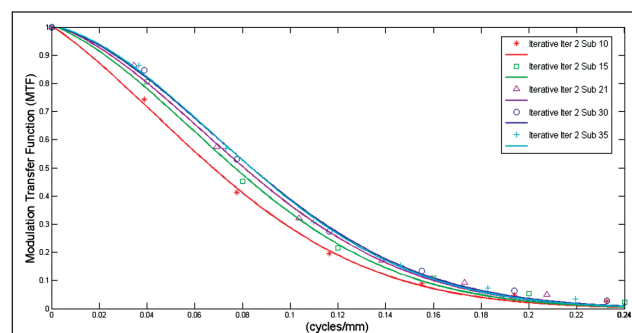


Figure 8. 3D scanning and the effect of different subsets into the MTF. MTF obtained with the LSF method from PET images using the plane source method, 3D scanning and iterative reconstruction algorithms with 2 iterations.

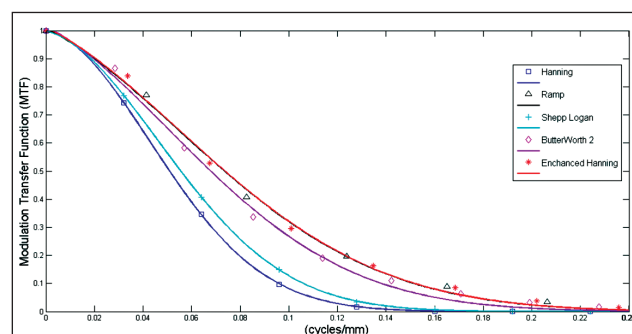


Figure 9. Modulation transfer function, obtained with the LSF method from PET images using the plane source method and 2D scanning with different filters. The filters are: Hanning, Ramp, Shepp Logan, ButterWorth 2 and Enhanced Hanning.

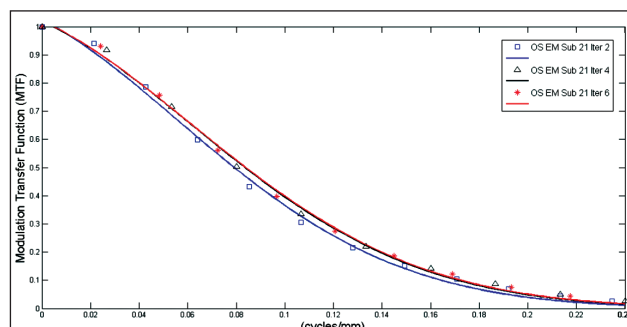


Figure 10. 2D scanning and the effect of different iterations into the MTF. MTF obtained with the LSF method from PET images using the plane source method, 2D scanning and OS EM reconstruction algorithm with 21 subsets.

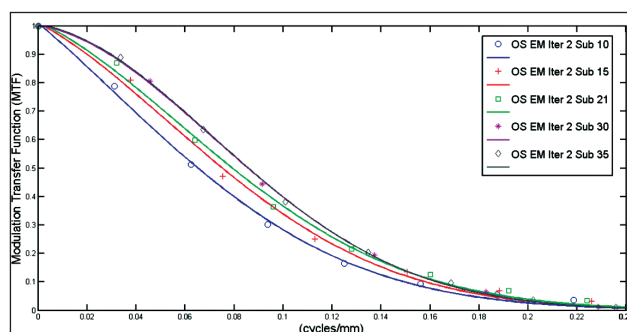


Figure 11. 2D scanning and the effect of different subsets into the MTF. MTF obtained with the LSF method from PET images using the plane source method, 2D scanning and OS EM reconstruction algorithm with 2 iterations.

6. In Figure 11, the reconstruction algorithm was OS EM with 2 iterations, while subsets ranged from 10 to 35.

All MTF were obtained after the selection of the LSF fitting, providing the optimum RMSE and R2 value. For the standard whole body PET protocols of the scanner, in 3D and 2D scanning mode, the optimum LSF fitting function and the corresponding RMSE and R2 values are listed in Table 2.

Figures 7 and 10 show that while low and high frequency response is similar, there are differences in the middle frequency area as the iterations increase, for both 3D iterative and 2D OS EM reconstruction algorithms respectively.

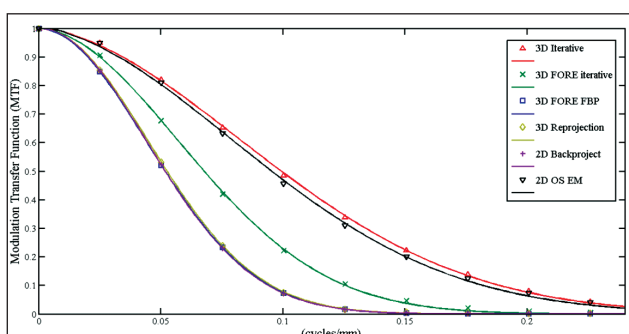
Figures 8 and 11 show that low and middle frequencies are affected with subsets change in 3D iterative and 2D OS EM kernels respectively. Increasing the number of subsets, from 10 up to 30, results in increased contrast for the lower and the middle frequency features in both cases. Further increase, from 30 to 35, has less effect as shown by the MTF. For the higher frequency features in the image, subsets change seems to have little effect.

Figure 12 shows MTF results, obtained with the PSF method from PET images, in transverse plane, using the standard whole body PET protocols of the scanner in 3D and 2D scanning mode. The MTF were obtained after the selection of the PSF fitting providing the optimum RMSE and R2 value. These values are listed in Table 3.

In Figure 12 the curve showing the highest MTF values was obtained for the Iterative with 2 iterations and 30 subsets reconstruction method for a 3D scanning protocol. The 2D backprojection reconstruction method, with Hanning fil-

Table 2. LSF optimum fitting method used in MTF calculation in Figures 6-11

Optimum fitting for the LSF method				
PET Protocol	Reconstruction method	Goodness of fit parameters		Fitting
		RMSE	(R ²)	
3D	Reprojection	0.2747	0.9998	Lorentzian & Gaussian
	FORE FBP	0.4117	0.9962	Sum of two Gaussians
	FORE Iterative	0.3426	0.9998	Lorentzian & Gaussian
	Iterative	0.3923	0.9953	Sum of two Gaussians
2D	Backproject	0.4642	0.9996	Sum of two Gaussians
	OS EM	0.3214	0.9996	» » » »


Figure 12. Modulation transfer functions, obtained with the PSF method from PET images using the 3D and 2D scanning protocols.

ter (cut-off frequency 10.9), had the lowest MTF in the range of spatial frequencies with a stopband edge in MTF of 0.17 cycles/mm. The effect of the filters, iterations and subsets on the MTF was similar as in the case of the LSF method.

As seen in Figure 12, the use of an iterative reconstruction algorithm leads to qualitative and quantitative improvements in image quality, regardless the scanning method. Furthermore, MTF of the 2D OS EM and 3D iterative algorithms are comparable. This is also the case for the MTF of the 3D FORE FBP and 2D backprojection reconstruction algorithms.

Figure 12 pinpoints that the main improvement to the PET imaging has resulted by the introduction and use of iterative reconstruction algorithms.

The advantages of iterative algorithms can be seen in Figure 13, where clinical images of: a) abdomen, scanned in 3D mode and b) brain, scanned in 2D mode, are presented. Images were reconstructed with conventional and iterative algorithms. In both modes, the application of iterative reconstruction improves quality, as seen by image resolution.

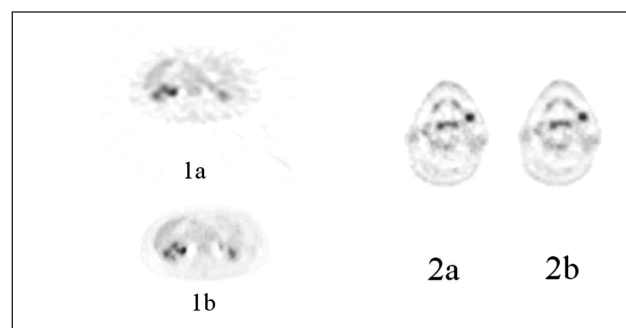
Discussion

The PSF contains complete information about the spatial resolution. On the other hand, in order to express the spatial resolution we usually ignore the shape of the PSF and simply

Table 3. PSF optimum fitting method used in MTF calculation in Figure 12

Optimum fitting for the PSF method				
PET Protocol	Reconstruction method	Goodness of fit parameters		
		RMSE	(R ²)	
3D	Reprojection	0.5220	0.9998	
	FORE FBP	0.5608	0.9998	
	FORE Iterative	0.2679	0.9999	
	Iterative	0.3014	0.9999	
2D	Backproject	0.5244	0.9998	
	OS EM	0.3181	0.9999	

* In all, fitting was the sum of two Gaussians


Figure 13. Clinical images scanned in different modes and reconstructed with different algorithms. Left: 1a. Abdomen 3D reprojection, 1b. Abdomen 3D iterative. Right: 2a. Brain 2D backprojection, 2b. Brain 2D OS EM.

measure its width. Unfortunately, this method has significant drawbacks. Another way to measure image resolution is by looking at the frequency response. Taking the 2D Fourier transform of the PSF provides the 2D frequency response. If the PSF is circularly symmetric, its frequency response will also be circularly symmetric. In this case, complete information about the frequency response is contained in its profile. In cases where the PSF is not circularly symmetric, the entire 2D frequency response contains information regarding resolution since its line profile depends on the angle [32].

A more favorable alternative is the LSF. Its advantage is that the MTF can be directly found by taking the 1D FFT of the LSF (unlike the PSF to MTF calculation that must use a 2D Fourier transform). If a system has an oblong PSF, its spatial resolution will be different in the vertical and horizontal directions, resulting in LSF different in these directions [32]. Measuring the LSF in the vertical and horizontal directions makes it possible to describe the non-circular PSF more accurately.

The MTF of a line source is the equivalent of the LSF in the spatial frequency domain where signals can be easily decomposed into sine waves. In this way the signal obtained from the plane source can provide useful information concerning the signal amplitude, frequency and phase of object signals passing through the imaging system. For each spatial frequency (which corresponds to a particular object size in the space domain) MTF gives the corresponding amplitude of useful signal, i.e. the contrast level in the final image of the particular object size. A single MTF analysis in the spatial frequency domain can be used to predict the system performance for all possible structure sizes.

The MTF can also be used to quantify an imaging system's ability to recover an input contrast at a certain spatial frequency [33]. A system with a flat MTF curve having a value near unity (spatial frequency) would faithfully reproduce the image object with high-contrast recovery. MTF curves can be evaluated to reveal contrast improvement under factors that affect contrast recovery such as spatial resolution improvement, object size, scattering and random coincidence events.

The differences between the PSF and LSF methods, in the MTF calculation, could be attributed to the fact that ideal points and lines cannot be employed under experimental conditions and to that iterative algorithms are not linear [34]. The LSF method employed here uses more data than the corresponding PSF, because a line is used instead of a point. For this reason, this method is less prone to noise due to the benefits of averaging larger amount of data by using more samples (line profiles) [8]. Thus, our method regarding the MTF calculation of the PET images provided a mean standard deviation of $\overline{sd} = 0.0043$, in contrary to the PSF method, which showed $sd = 0.0405$. This may be the principal benefit of the proposed method in the context of clinical PET MTF measurements.

Point sources in glass capillaries free in air could be affected by the range of the positrons emitted by the source due to the finite source size, whereas methods that use phantoms as attenuation media do not exhibit this dependence. Measuring spatial resolution from a sharp interface (such as the plane source presented here) that produces a plane response function may become increasingly important as the spatial resolution of PET systems improves. Such measurements have been widely investigated in other areas of medical imaging. Examples of similar work can be also found in computed tomography (CT) [8, 13], single photon emission tomography (SPET) [12] and PET/ magnetic resonance imaging (MRI) [35].

The method presented in this work provides the ability to obtain image resolution in three axes by placing the source only horizontally and vertically. In addition, a significant number of pixels, over the entire LSF, are averaged to estimate the MTF. This is an advantage since the point sources appearing in PET images of 256X256 dimensions, will incorporate only a few pixels, which may be insufficient to correctly characterize image contrast [36].

Decreasing MTF at higher frequencies causes the blurring of high frequency features in an image. This blurring was a characteristic of the older 2D reconstruction algorithm (backprojection). The new fully 3D iterative reconstruction algorithm is superior in contrast and resolution as seen by its MTF. Since PET is an intrinsic 3D imaging modality, it will benefit by the 3D algorithms.

The requirements for measuring the MTF of an imaging system include: a) a linear signal response and b) a shift invariant signal (i.e., signal independent of location in the image). In the strictest sense of the definition, most imaging systems are nonlinear and shift-variant. Furthermore most clinical systems incorporate iterative reconstruction algorithms which are non-linear and difficult to evaluate [32, 37]. It is important to attempt to evaluate these systems by using certain experimental conditions under which linearity and shift-invariance can be a reasonable assumption. These con-

ditions often include low-contrast and localized measurements. As a result, it is often necessary to specify under which conditions the MTF results are valid. Measurement of MTF for a nonlinear system has been the focus of past research and was employed to predict the detectability index for detection and discrimination tasks [13, 38, 39]. Similarly, in this work, the MTF was measured under predefined conditions such as field of view, contrast and noise levels. This yielded a specific task-based transfer function that can be used to compute performance assessment metrics such as the detectability index. This work is further justified by the need to define the MTF on a locally linearizable region of the object, to assess the task-specific performance in the presence of nonlinear reconstruction algorithms.

The reconstruction algorithm strongly affects the image characteristics (Fig. 12), however manufacturers generally do not divulge the actual shape of the reconstruction kernels. Furthermore, image reconstruction algorithms are not included in the tests of acceptance [4]. The determination of a scanner's MTF provides an easy means to evaluate the frequency response of each kernel available [8]. The MTF method used, could be useful for comparing the effects of different scanning modes and reconstruction parameters (2D vs 3D, FBP vs OSEM, etc) [10, 11] and for the evaluation of fine details in PET imaging, albeit under very specific imaging conditions and despite algorithm nonlinearities. Additionally it can be used for accurate image resolution determination of scanners incorporating high resolution detectors [40, 41].

The above advantages of the MTF method presented may be valuable in clinical practice. The need for common clinical and technical standards in PET/CT is an actual demand, as in multicenter trials it is not possible to image all patients with the same PET/CT system. Nowadays, there is an increasing interest in studies concerning the early assessment of treatment response in the course of chemotherapy or radiotherapy in patients with tumors of different types. A major problem in these studies is the comparability of quantitative PET results, usually expressed as standardized uptake values (SUV) and calls into question the general use of SUV cut-off values in clinical routine or clinical trials. MTF may be able to restore comparability between data sets from different PET systems and lead to a reduction in data variability [42].

Assessment of the line spread function and hence modulation transfer function (MTF) can be used in preprocessing operations to compensate for the image degradation. This could result in improvement in image quality since these new algorithms will incorporate event physics detection [43]. Subsequently MTF could also be applicable for dose reduction to essential levels, especially when dosimetry on pre-treatment scans in terms of target and dose-limiting tissue uptake determination for optimal targeted radionuclide treatment conditions is needed [44].

The use of MTF provides a mean to visualize the outcome of the image formation. This could provide a common language between physicians and physicists. Most physicians feel that the mathematics involved into the reconstruction processes are beyond their scientific interests. On the contrary many are aware that, the MTF quantifies how well a subject's regional brightness variations are preserved when

they pass through an imaging system, from other commercial uses of imaging. The matching of the image outcome with reconstruction via its corresponding MTF, as seen by comparing Figures 12 and 13, could help the physicians become more familiar with imaging.

Assessment of a PET system performance through the MTF could be valuable, since the acquisition and processing protocols could be optimized prior to their use in clinical practice. Furthermore, since spatial resolution is usually characterized by the MTF, the diagnostic capabilities of the system could also be evaluated.

A highly sensitive quality assurance (QA) methodology is essential to appropriately assess performance and performance stability of a PET/CT system during clinical use. Routine QA measurements of MTF, provide an effective method to quantify any loss in image quality that may be induced during every day clinical practice use such as mechanical damage, misalignments, inappropriate calibration, mistimed gating sequences, and damage to system electronics. Image MTF measurements can be used as an overall quality assurance method that is sensitive to many system parameters. If MTF changes occur, more specific tests should be implemented to identify the cause of the problem. Moreover, QA measurements of MTF can be more effectively compared to other clinical systems as well as reported measurements of research prototypes, even if such comparisons include the possible effects of varying characteristics. In this case, the ability to compare clinical image quality with the theoretical upper limits usually demonstrated with research prototypes could be useful in evaluating possible effects of the choice and/or quality of the PET system. Our methodology is suited for clinical QA as well as research and development of prototype imagers. The robustness and accuracy of linear - under specific imaging conditions- systems metrics and the simplicity of the plane source make this method an invaluable tool to ensure optimal image quality.

The limitations of the MTF calculation, through the PSF method, arise from the fact that the PSF has a complicated, non-separable 3D shape. Following the assumption of rotational symmetry, the PSF profiles could be averaged in radial directions as has been reported for spiral CT [45]. Possible disadvantages of the plane source LSF method in comparison with the point source PSF could be scatter and streak artifacts. In this sense the plane source LSF method could be considered as more realistic, with respect to clinical practice, since both scattering and streak artifacts are present in PET in vivo clinical imaging.

Our study is related to its application to only one PET system; therefore, the MTF was measured only for the types of iterative reconstructions that were installed into it. There are many parameters in iterative reconstructions, such as the regularizer and edge preservers, that could affect the MTF. Therefore, the MTF results shown in this work are representative only of the conditions used in this study. Future studies are warranted to include other PET system and reconstruction algorithms as well as the dependence of MTF in iterative reconstruction images with contrast.

In conclusion, the modulation transfer function, important for the characterization of the spatial resolution of a positron emission tomography (PET) system, was determined by the

LSF method. This method is based on a novel thin plane source, which was prepared in our laboratory by immersing Al substrate chromatography paper, in ^{18}F -FDG radiopharmaceutical solution. The method presented in this work can be used for comparing clinical reconstruction protocols and as a quality control method to identify the system's performance and stability. The novel thin plane source is easy to prepare and can be implemented with low cost materials available at a nuclear medicine laboratory.

The authors declare that they have no conflicts of interest.

Bibliography

1. Rahmim A, Qi J, Sossi V. Resolution modelling in PET imaging: theory, practice, benefits, and pitfalls. *Med Phys* 2013; 40: 064301 1-15.
2. Alessio AM, Rahmim A, Orton CG. Resolution modelling enhances PET imaging. *Med Phys* 2013; 40: 120601 1-4.
3. Tyson RK, Amtey SR. Practical considerations in gamma camera line spread function measurement. *Med Phys* 1978; 5: 480-4.
4. NEMA standards publication NU 2-2001: Performance measurements of positron emission tomographs. *Technical report National Electrical Manufacturers Association*, Washington, DC, 2001; 7-10.
5. Bischof CL, Ehrhardt JC. Modulation transfer function of the EMI CT head scanner. *Med Phys* 1977; 4: 163-7.
6. Nickoloff EL, Riley R. A simplified approach for modulation transfer function determinations in computed tomography. *Med Phys* 1985; 12: 437-42.
7. Droege RT, Morin RL. A practical method to measure the MTF of CT scanners. *Med Phys* 1982; 9: 758-60.
8. Boone JM. Determination of the presampled MTF in computed tomography. *Med Phys* 2001; 28: 356-60.
9. Ohkubo M, Wada S, Matsumoto T et al. An effective method to verify line and point spread functions measured in computed tomography. *Med Phys* 2006; 33: 2757-64.
10. Kachelriess M, Kalender WA. Presampling, algorithm factors, and noise: Considerations for CT in particular and for medical imaging in general. *Med Phys* 2005; 32: 1321-34.
11. Flohr TG, Stierstorfer K, Ulzheimer S et al. Image reconstruction and image quality evaluation for a 64-slice CT scanner with z-flying focal spot. *Med Phys* 2005; 32: 2536-47.
12. Fountos G P, Michail CM, Zanglis A et al. A novel easy-to-use phantom for the determination of MTF in SPECT scanners. *Med Phys* 2012; 39(3): 1561-70.
13. Richard S, Ravin CE, Husarik DB et al. Towards task-based assessment of CT performance: System and object MTF across different reconstruction algorithms. *Med Phys* 2012; 39(7): 4115-22.
14. Starck S, Bath M, Carlsson S. The use of detective quantum efficiency (DQE) in evaluating the performance of gamma camera systems. *Phys Med Biol* 2005; 50: 1601-9.
15. Beck RN. The Scanning System as a Whole: General considerations. In: Gottschalk A, Beck RN, *Eds Fundamental Problems in Scanning*. Charles C Thomas Publisher, Springfield, Illinois, 1968; p 17.
16. Beck RN, Zimmer LT, Charleston DB et al. Advances in fundamental aspects of imaging systems and techniques. In: *Medical Radioisotope Scintigraphy Vol I* 1972; p 3-45. Proceedings of a symposium on Medical Radioisotope Scintigraphy held by the International Atomic Energy Agency in Monte Carlo, 23-28 October 1972, IAEA, Vienna, 1973.
17. Tsialas SP, Psarrakos KP. Experimental methods for determining the septum penetration of focused collimators. In: *Medical Radioisotope Scintigraphy Vol I* 1972; p 47-59. Proceedings of a symposium on Medical Radioisotope Scintigraphy held by the International Atomic Energy Agency in Monte Carlo, 23-28 October 1972, IAEA, Vienna, 1973.
18. van Staden JA, du Raan H, Lötter MG et al. Production of radioactive quality assurance phantoms using a standard inkjet printer. *Phys Med Biol* 2007; 52: N329-N337.
19. Fujita H, Tsia D, Itoh T et al. A simple method for determining the modulation transfer function in digital radiography. *IEEE Trans Med*

- Imaging* 1992; 11: 34-9.
20. Santos J, Sarmiento S, Alves P et al. Single-acquisition method for simultaneous determination of extrinsic gamma-camera sensitivity and spatial resolution. *Appl Rad Isot* 2008; 66(1): 44-9.
 21. Cunningham IA. Applied Linear Systems theory. In Beutel J, Kundel HL, Van Metter RL, Eds. *Handbook of Medical Imaging: Physics and Psychophysics*. SPIE, Bellingham, WA, 2000, Vol. 1, pp. 79-161.
 22. Greer PB, van Doorn T. Evaluation of an algorithm for the assessment of the MTF using an edge method. *Med Phys* 2000; 27(9): 2048-59.
 23. Ohkubo M, Wada S, Kayugawa A et al. Image filtering as an alternative to the application of a different reconstruction kernel in CT imaging: Feasibility study in lung cancer screening. *Med Phys* 2011; 38(7): 3915-23.
 24. Dougherty G, Newman D. Measurement of thickness and density of thin structures by computed tomography: a simulation study. *Med Phys* 1999; 26: 1341-8.
 25. Prevrhal S, Engelke K, Kalender WA. Accuracy limits for the determination of cortical width and density: the influence of object size and CT imaging parameters. *Phys Med Biol* 1999; 44: 751-64.
 26. Prevrhal S, Fox JC, Shepherd JA et al. Accuracy of CT-based thickness measurement of thin structures: modeling of limited spatial resolution in all three dimensions. *Med Phys* 2003; 30: 1-8.
 27. Vu Nam T, Silverman RW, Chatziioannou AF. Preliminary performance of optical PET (OPET) detectors for the detection of visible light photons. *Nucl Instrum Methods Phys Res A* 2006; 569: 563-6.
 28. Mettivier G, Russo P. Measurement of the MTF of a Cone-Beam Breast Computed Tomography Laboratory Scanner. *IEEE Trans Nucl Sci* 2011; 58(3): 703-13.
 29. Erhardt JC. Reduction of aliasing in modulation transfer function measurements. *Med Phys* 1986; 13: 658-62.
 30. Dougherty G, Newman D. Measurement of thickness and density of thin structures by computed tomography: A simulation study. *Med Phys* 1999; 26: 1341-8.
 31. Koral KF, Kritzmaan JN, Rogers VE et al. Optimizing the number of equivalent iterations of 3D OSEM in SPECT reconstruction of I-131 focal activities. *Nucl Instrum Methods Phys Res A* 2007; 579: 326-9.
 32. Smith SW. *The Scientist and Engineer's Guide to Digital Signal Processing*. 2nd edn California Technical Publishing 1999; 423-30.
 33. Sorenson J, Phelps ME. *Physics in Nuclear Medicine*. 2nd edn, New York: Saunders 1986; 367-9.
 34. Kaftandjian V, Zhu YM, Roziere G et al. A Comparison of the Ball, Wire, Edge, and Bar/Space Pattern Techniques for Modulation Transfer Function Measurements of Linear X-Ray Detectors. *J X-Ray Sci Tech* 1996; 6(2): 205-21.
 35. Peng H, Levin CS. Study of PET intrinsic spatial resolution and contrast recovery improvement for PET/MRI systems. *Phys Med Biol* 2012; 57: N101-15.
 36. Prevrhal S, Engelke K, Kalender WA. Accuracy limits for the determination of cortical width and density: the influence of object size and CT imaging parameters. *Phys Med Biol* 1999; 44: 751-64.
 37. Levin CS, Hoffman EJ. Calculation of positron range and its effect on the fundamental limit of positron emission tomography system spatial resolution. *Phys Med Biol* 1999; 44: 781-99.
 38. Samei E, Badano A, Chakraborty D et al. *Assessment of display performance for medical imaging systems*. Report of the American Association of Physicists in Medicine (AAPM) Task Group 18, 2005.
 39. Richard S, Siewerdsen JH. Cascaded systems analysis of noise reduction algorithms in dual-energy imaging. *Med Phys* 2008; 35(2): 586-601.
 40. Soret M, Bacharach SL, Buvat I. Partial-Volume Effect in PET Tumor Imaging. *J Nucl Med* 2007; 48: 932-45.
 41. Parka SJ, Rogers WL, Huh S et al. A prototype of very high resolution small animal PET scanner using silicon pad detectors. *Nucl Instrum Methods Phys Res A* 2007; 570(3): 543-55.
 42. Prenosil GA, Weitzel T, Hentschel M et al. Transconvolution and the virtual positron emission tomography - a new method for cross calibration in quantitative PET/CT imaging. *Med Phys* 2013; 40: 062503 1-15.
 43. Brix G, Doll J, Bellemann ME et al. Use of scanner characteristics in iterative image reconstruction for high-resolution positron emission tomography studies of small animals. *Eur J Nucl Med* 1997; 24: 779-86.
 44. Grammaticos P, Fountos G. The physician should benefit, not harm the patient. *Hell J Nucl Med* 2006; 9(2): 82-4.
 45. Dainty JC, Shaw R. *Image Science* (Academic Press, London, 1974); 267-82.